Biochemical and Biophysical Research Communications 445 (2014) 463–468

Contents lists available at ScienceDirect

Biochemical and Biophysical Research Communications

journal homepage: www.elsevier.com/locate/ybbrc

Regulation of channel function due to physical energetic coupling with a lipid bilayer

Md. Ashrafuzzaman [a,*], C.-Y. Tseng [b,1], J.A. Tuszynski [b,c]

[a] Department of Biochemistry, College of Science, King Saud University, Riyadh 11451, Saudi Arabia
[b] Department of Oncology, University of Alberta, Edmonton, Canada
[c] Department of Physics, University of Alberta, Edmonton, Canada

ARTICLE INFO

Article history:
Received 29 January 2014
Available online 12 February 2014

Keywords:
Lipid bilayer
Ion channel
Membrane protein
Screened Coulomb interaction
MD simulations

ABSTRACT

Regulation of membrane protein functions due to hydrophobic coupling with a lipid bilayer has been investigated. An energy formula describing interactions between lipid bilayer and integral ion channels with different structures, which is based on the screened Coulomb interaction approximation, has been developed. Here the interaction energy is represented as being due to charge-based interactions between channel and lipid bilayer. The hydrophobic bilayer thickness channel length mismatch is found to induce channel destabilization exponentially while negative lipid curvature linearly. Experimental parameters related to channel dynamics are consistent with theoretical predictions. To measure comparable energy parameters directly in the system and to elucidate the mechanism at an atomistic level we performed molecular dynamics (MD) simulations of the ion channel forming peptide–lipid complexes. MD simulations indicate that peptides and lipids experience electrostatic and van der Waals interactions for short period of time when found within each other's proximity. The energies from these two interactions are found to be similar to the energies derived theoretically using the screened Coulomb and the van der Waals interactions between peptides (in ion channel) and lipids (in lipid bilayer) due to mainly their charge properties. The results of *in silico* MD studies taken together with experimental observable parameters and theoretical energetic predictions suggest that the peptides induce ion channels inside lipid membranes due to peptide–lipid physical interactions. This study provides a new insight helping better understand of the underlying mechanisms of membrane protein functions in cell membrane leading to important biological implications.

1. Introduction

Membrane protein conformational changes can be reflected through opening/closing transitions in lipid bilayer hosted ion channels [1]. In many such cases a bilayer perturbation occurs near proteins [2] (see Supp Fig. 1). The bilayer possessing elastic properties [3] incurs an energetic cost $\Delta G^0_{\mathrm{def}}$ which contributes to the overall free energy difference $\Delta G^{\mathrm{I}\to\mathrm{II}}_{\mathrm{tot}} = \Delta G^{\mathrm{I}\to\mathrm{II}}_{\mathrm{prot}} + \Delta\Delta G^{\mathrm{I}\to\mathrm{II}}_{\mathrm{def}}$ between two protein states e.g., I and II. The free energy contribution $\Delta G^{\mathrm{I}\to\mathrm{II}}_{\mathrm{prot}}$ is the energetic cost of the protein conformational change *per se* and $\Delta\Delta G^{\mathrm{I}\to\mathrm{II}}_{\mathrm{def}}$ is the bilayer deformation energy difference between two states. In this bilayer-protein interaction, bilayer deformation appears to be a regulator of integral membrane protein functions. To understand this phenomenon, we experimentally and theoretically investigate how lipid membranes with different mechanical, geometrical and electrical properties regulate the integral ion channel energetics using two structurally different channels, namely β-helical gramicidin A (gA) [4] and 'barrel-stave' pore type alamethicin (Alm) [5,6] (Supp Fig. 1).

Molecular mechanisms of peptide effects on membranes have been investigated especially by performing molecular dynamics (MD) simulations of both peptides gA- and Alm-lipid complexes. Here we report computational results for any possible peptide–lipid physical interactions, which might play crucial roles behind the creation of stable ion channels that are hydrophobically coupled to host bilayers. We specifically focus on the peptide–lipid binding energies and parameters related to stability of the complex. These MD results also shed new light on the complex interactions between stable structure (e.g., biomolecules) and liquid crystal structure (e.g., membrane), a very important and still unresolved problem in biophysics and soft condensed matter physics.

* Corresponding author.
E-mail address: mashrafuzzaman@ksu.edu.sa (Md. Ashrafuzzaman).
[1] CYT is currently with Sinoveda Canada Inc, Edmonton, AB, Canada.

http://dx.doi.org/10.1016/j.bbrc.2014.02.012
0006-291X/

The MD simulation was initiated based on a strong background of theoretical and experimental understanding of the phenomenological aspects of the problem. In gA channel formation the association of two trans-bilayer gA monomers is governed by the dimerization coefficient: $K_D = [D]/[M_g]^2 = k_1/k_{-1} = \exp\left\{-\left(\Delta G^0_{prot} + \Delta G^0_{def}\right)/k_B T\right\}$, where $[M_g]$ and $[D]$ are monomer and dimer concentrations; and k_1 and k_{-1} are rate constants determining the gA channel appearance rate ($f_g = k_1 \cdot [M_g]^2$) and lifetime ($\tau = 1/k_{-1}$) [7]. k_B and T are the Boltzmann constant and absolute temperature, respectively. Since the bilayer deformation energy ΔG^0_{def} is sensitive to the hydrophobic mismatch ($d_0 - l$) between bilayer thickness (d_0) and gA channel length (l), the bilayer responds to its deformation by imposing a restoring/channel-dissociation force F_{dis} on the edges of a channel [7–9]. Increasing F_{dis} is reflected in a decreasing τ and vice versa, channels thus become molecular force transducers [7]. Within limits, the channel structure can be considered invariant when d_0 is varied [10], meaning gA channel is more rigid than a lipid bilayer. All-atom MD simulations of gA in bilayers [11] show how lipid head groups organize themselves in the region of hydrophobic free length $d_0 - l$. Potential-of-mean-force calculations [12] suggest that trans-membrane protein interactions are regulated by a hydrophobic mismatch equivalent to $d_0 - l$. The calculation of F_{dis} has been a long-standing challenge. Based on a well-established theory of elastic bilayer (EB) deformation [13] ΔG^0_{def} has been found to be approximately changing as a quadratic function of $d_0 - l$ [13,14] but subsequent developments [15–18] resulted in introduction of lipid intrinsic curvature c_0 (whose positive and negative changes correspond to increases and decreases of the hexagonal lipid phase, respectively, and any such local curvature profile generally controls the lipid packing energy profiles in bilayers) [19] into the expression for ΔG^0_{def} which is now considered to be a quadratic function of $d_0 - l$ and intrinsic curvature c_0, $\Delta^0_{def} = H_B \cdot (d_0 - l)^2 + H_X \cdot (d_0 - l) \cdot c_0 + H_c \cdot c_0^2$. Consequently, F_{dis} changes linearly with $d_0 - l$ and c_0 [7,8]: $F_{dis} = -(-(\partial/\partial(d_0 - l))\Delta G^0_{def}) = 2H_B \cdot (d_0 - l) + H_X \cdot c_0$. Here H_B, H_X and H_c are phenomenological elastic constants. Using 'elastic parameters' in a fluid-like membrane is a good first-order approximation that works well within the limitations of a linear theory. To extend the applicability of the theory to a nonlinear regime, we use the 'screened Coulomb interaction' (SCI) [9,20]. The interaction energy between a gA channel and a host bilayer has been calculated based on experimentally observable parameters such as d_0 [21], lipid head group dimension [22], l [21], lipid charge q_L [23] and dielectric parameters of the lipid bilayer core [24]. Considering $l < d_0$, the channel extends its Coulomb interaction towards lipids placed at the bilayer's nearest resting thickness (Supp Fig. 1). A gA channel directly interacts with a nearest-neighbor lipid by Coulomb forces and this lipid interacts directly with the next-nearest-neighbor lipid but this second lipid's interaction with the channel is screened by the channel's nearest-neighbor lipid. The interaction between the third-nearest neighbors and the channel is screened by the lipids in between. The general form of SCI is:

$$V_{sc}(\vec{r}) = \int d^3k Exp\{i\vec{k} \cdot \vec{r}\} V_{sc}(\vec{k}) \quad (1)$$

whose Fourier transform is [25]:

$$V_{sc}\left(\vec{k}\right) = \frac{V(\vec{k})}{1 + \frac{V(\vec{k})}{2\pi k_B T} n} \quad (2)$$

where $V(k) = (1/\varepsilon_0 \cdot \varepsilon_r) q_g q_L / k^2$ is the direct Coulomb interaction between a gA monomer (with a charge q_g) in a channel and the nearest-neighbor lipid. $k \approx 2\pi/r_{LL}$, r_{LL} is the average lipid–lipid distance [22], assumed also be the distance between the channel's longitudinal edge and the nearest lipid head group. n Is lipid density $\sim$1/60 Å^2. Obviously, $k_B T \approx 1.38 \times 10^{-23}$ J/K (300 K). Here, ε_0 is the dielectric constant in vacuum and ε_r ($\sim$2) is the relative dielectric constant inside the membrane [24] where all peptide–lipid interactions are assumed to take place.

Theoretical calculation of a channel's energies and their direct correlation with experimentally observable channel stability. The binding energy between two monomers in a gA channel ($U_{g,g}$) is due to the Lennard–Jones and Coulomb potentials [26]. gA channel stability τ does not primarily follow the modest change in $U_{g,g}$ due to change of gA monomer's charge profile which has been found valid in case of binding of amphiphiles, anti-fusion and AMPs with channels in a varied membrane environment (manuscript in preparation). Monomer–monomer binding in a gA channel is therefore comparatively very rigid. These observations together with those presented in [10] suggest that a change in τ is mainly due to the change in the gA channel bilayer coupling energy ($U_{g,bilayer}$) even though the total binding energy is $U(r) = U_{g,g} + U_{g,bilayer}$. Here, $U_{g,bilayer}$ is proportional to the 1st, 2nd, etc. order term in the expansion of $V_{sc}(r)$ for the hydrophobic mismatch to be filled by single, double etc. lipids representing 1st, 2nd, etc. order screening, respectively (details in [9,20]). ΔG^0_{prot} and ΔG^0_{def} are proportional to $U_{g,g}$ and $U_{g,bilayer}$, respectively. These energies can be detected using MD simulation. F_{dis} therefore originates from mechano-electrical properties of membranes [9,20].

2. Materials and methods

Detailed materials and methods for numerical computation and experimental techniques are [9,20]. To address SCI's various lipid order screening $d_0 - l$ was experimentally [9] varied by changing d_0 using lipids with varying acyl chain length or gA monomers of different lengths or both, which changes F_{dis} and as a result τ (see Supp Fig. 2). Addition of phosphoethanolamine fractionally with phosphocholine introduces negative curvature [19] in bilayer with comparable d_0 [27]. Further parametric information in peptide-membrane interactions can be obtained in various places e.g., [28–32].

For MD simulations to investigate AMP–lipid interactions in molecular level we modeled dynamical changes of *in silico* peptide–lipid interactions following the protocol used *in silico* modeling of CD–lipid interactions [33]. Based on Monte Carlo concept, we considered five different relative locations and orientations randomly generated in each AMP–lipid complex as initial structures for MD simulations to increase sampling size for better statistical analysis. For each location- and orientation-specific complex, a 10 ns explicit water MD simulation at temperature 300 K in an aqueous solution at pH 7 was performed. We applied the software package Amber 11 (Amber force field ff03) [34]. The explicit water TIP3P model was used to simulate solvent effects. The force field parameters for AMPs and lipids (PC and PS) were generated using an Amber module antechamber [35,36]. The parameters for AMPs were compared with those generated for colchicine [37] and taxol [38] respectively. Both studies [37,38] have shown these parameterizations lead to simulations that are consistent with experiments. Therefore, similar results based on these parameterizations are expected. In simulation, first, twenty complexes were energy minimized using the steepest descent method for the first ten cycles and then followed by a conjugate gradient for another 1000 cycles. We then applied Langevin dynamics during the process of heating up the system for 200 ps with the energy minimized complex, in which AMP and lipid molecules were being restrained using a harmonic potential with a force constant $k = 100$ N/m. Afterward, we introduced pressure regulation to equilibrate water molecules around the complex and to reach an

equilibrium density for another 200 ps in addition to temperature regulation. The MD production run then was continued for 10 ns. Given five various initial structures for each AMP–lipid pair, a total 50 ns simulation result was analyzed to gain insights into the direct interactions of the corresponding pair. Note that the lipid was gently restrained with a harmonic potential with a force constant k = 10 N/m, applied only to the phosphate during the production runs. The purpose of this restraint is to mimic a single lipid being "restrained" in the membrane while both head group and two tails of such lipid still possess certain degrees of freedom.

3. Results and discussion

The experimental results suggest that $d_0 - l$ destabilizes (τ decreases) gA channel exponentially or to a higher order while negative increase of c_0 destabilizes it linearly (Supp Fig. 2 and in [9,20]). Moreover, f_g increases rapidly (to a second power or greater) with $[M_g]$, keeping τ constant. The required $[M_g]$ for considerable channel appearance rate f_g determines the change in ΔG^0_{def} [7]. The effects on f_g due to $d_0 - l$ are also reported to be greater than c_0 [9,20].

In SCI model calculations, GI increases rapidly with increasing screening order (Fig. 1). $\Delta G_{I,II} = G_I - G_{II}$ is the change in $U_{g,bilayer}$ which is equivalent to the free energy difference between free and dimer gA states assuming the change in ΔG^0_{prot} to be negligible. The result (Fig. 1) suggests, $\Delta G_{I,II} \propto e^{d_0 - l}$, so $F_{dis} = -(-\partial/\partial(d_0 - l)\ \Delta G_{I,II}) \propto e^{d_0 - l}$ [9,20].

$\tau \sim \exp\{-\Delta G_{I,II}/k_BT\} \sim \exp\{-\lambda\ F_{dis}/k_BT\}$ [7] where λ is the distance two gA monomers move apart to reach the dimer/monomer transition state [28]. $F_{dis} \sim \exp(d_0 - l)$ in the SCI model while $\sim(d_0 - l)$ in the EB model for unchanged c_0. In both cases the channel lifetime theoretically decreases exponentially at small $d_0 - l$ but as $d_0 - l$ increases, higher channel destabilization is observed in the former than in the latter case [9,20]. The origin of this difference is readily found if we expand the exponential expression (in the SCI model) in a power series as:

$\Delta G_{I,II} = \exp(d_0 - l) = \{(d_0 - l)^2/2\} + \{1 + (d_0 - l) + (d_0 - l)^3/6 + (d_0 - l)^4/24 + \ldots\} = \Delta G_{I,II}(\text{Harm}) + \Delta G_{I,II}(\text{A.Harm})$.

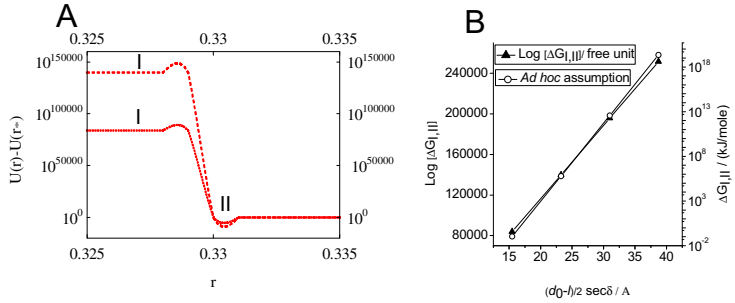

Fig. 1. (A) Energy (real part) vs. reaction coordinate (r) plot for gA channels (single and double dashed curves represent 1st and 2nd order screening, respectively) (using Eqs. 1 and 2). $r^* \approx 1.5$ Å (hydrogen bond length). I and II represent energy levels G_I and G_{II}, respectively, at which gA monomers exist as free and as dimmers, respectively. Assume $q_L/q_g = 0.005$, $(1/\varepsilon_0)q_Lq_g \approx 1$ (for simplicity), $r_{LL} = 7.74597$ Å [22]. Numerical integration was performed using Mathematica 7 ($-k_{max}2\pi/r_{LL}$, $k_{max}2\pi/r_{LL}$), $k_{max} = 100$, step size dr = 0.001 are judicious choices. In (B) $(d_0 - l)$ secδ is the distance covered by lipid head groups in the deformed bilayer region near channel. δ (~constant, within 0–90° in all screening orders) the angle at which lipids in the deformed portion couples with extension of channel length. With an *Ad hoc* assumptions ($q_g \sim$ electron charge and other relevant parameters), $\Delta G_{I,II}$(○)/(kJ/mole) seriously depends on q_L as d_0 increases.

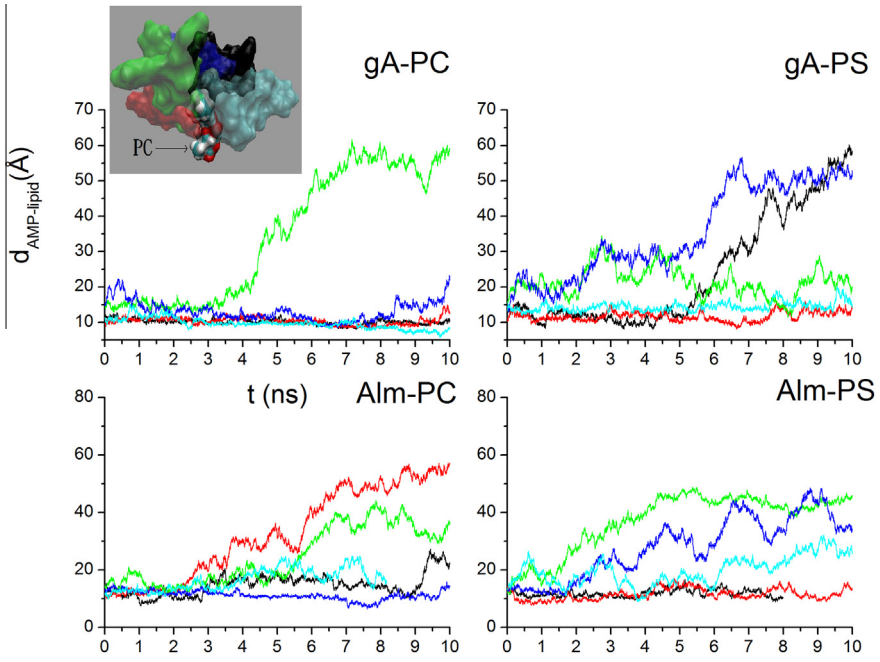

Fig. 2. MD simulation results representing the change in the AMP–lipid center of mass distance $d_{AMP-lipid}$ with time. Five curves with different colors represent five independent initial AMP–lipid complexes. The inset shows the cartoon representations of initial structures of five complexes with AMP following the color of the corresponding curve.

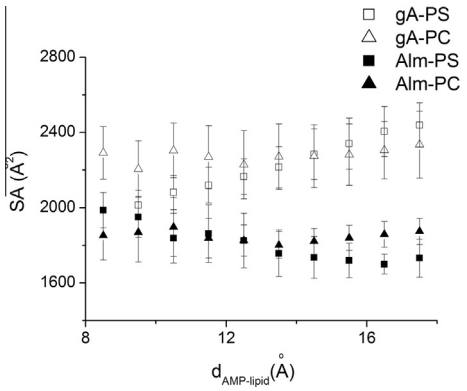

Fig. 3. SA areas for four complexes are plotted against $d_{AMP-lipid}$. It shows SA areas are fluctuating around 2300 and 1800 Å^2 for gA- and Alm-lipid respectively, which are independent of $d_{AMP-lipid}$.

Harm and A.Harm denote the harmonic and anharmonic contributions in $\Delta G_{I,II}$. The necessity to include $\Delta G_{I,II}$(A.Harm) is generally expected for higher $d_0 - l$ [see Supp Fig. 3]. The EB theory predicts the presence of only a harmonic term $\sim(d_0 - l)^2$ in the bilayer deformation energy which is adequate for sufficiently small deformation values and is also readily found in our screened Coulomb energy. Consequently, $F_{dis} = \partial/\partial(d_0 - l)\Delta G_{I,II}$ in the SCI model also contains additional terms (different orders) besides the term $\sim(d_0 - l)$ which is the only geometric mismatch term found in the EB theory to modulate the gA channel lifetime.

Although both SCI and EB model calculations generally suggest an exponential damping in the gA channel lifetime with increasing $d_0 - l$ which is consistent with the experimental data (Supp Fig. 2A and Ref. [8]), the SCI model calculation hints at the presence of extra damping due to higher order anharmonic terms in the energy expression. This may better explain why at high mismatch values, the channel experiences not just destabilization but also structural transitions mainly due to the cost of the super-heavy bilayer deformation energy (Fig. 1). We therefore conclude that although the EB model [13] which yields the deformation energy dependence according to $\sim(d_0 - l)^2$ [7,8] may be applicable in the small deformation limit, it requires a modification for larger deformation. For the same reason, the theory based on a linear spring approximation for the coupling between the bilayer and gA channels [29], which explicitly shows an exponential damping in τ with increasing $d_0 - l$, can be a good approximation when $d_0 - l$ is relatively small. However, for larger $d_0 - l$ when interaction between a gA channel with the bilayer extends to other next-neighbor lipids in the deformed regions of the bilayer near the channel, an extension of

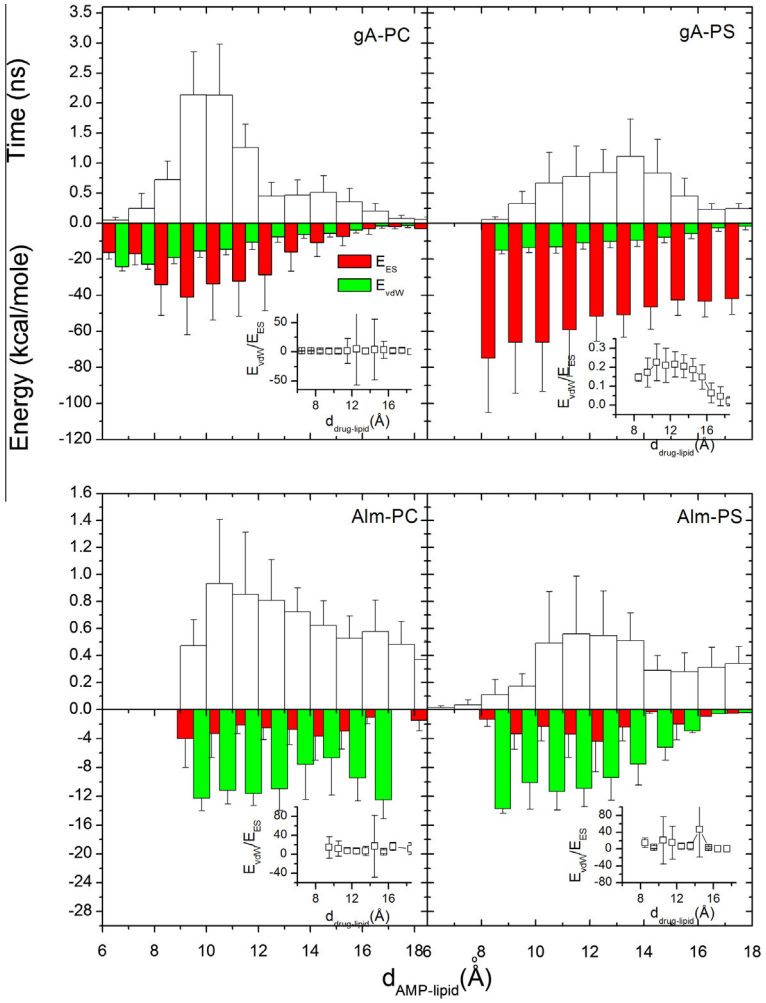

Fig. 4. In all four histogram plots (upper panel) of time vs. $d_{AMP-lipid}$, the time durations when AMP/lipid stay together (height) within a distance (width) during 10 ns simulations are presented. Lower panels show the histograms of non-bonded van der Waals (vdW) energy (E_{vdW}) and electrostatic (ES) interactions energy (E_{ES}). To avoid color conflict, E_{vdW} and E_{ES} are shown to occupy half–half widths, right-half and left-half respectively, although each half represents the whole width of the corresponding histogram.

EB model is needed. The SCI model calculation has provided such an extension. The SCI model also adequately explains the exponential damping nature of channel stability and even the structural transition of gA channels at any value of $d_0 - l$. Note, however, that the two approaches converge in the limit of small deformations. It is worth mentioning that in the case of considerable negative values of $d_0 - l$ (when $l > d_0$) the SCI should still be able to provide the major interacting components but since in this case the membrane–channel interaction energy causes a compression of the channels (opposite to pulling apart happening for positive $d_0 - l$), the monomer dissociation may also happen as a result of a planar shift and/or channel bending. The channel bending though is a result of the Coulomb interactions. The channel bending is however less likely to happen when uniform pulling forces are exerted on the channel by the bilayer from both longitudinal edges. An *ad hoc* assumptions on relevant parameters produces $\Delta G_{I,II}$/(kJ/mole) (Fig. 1, right panel) in the low $d_0 - l$ limit which is comparable to the value found in [7]. We therefore conclude that the regulation of membrane protein functions is due to the hydrophobic energetic coupling between the bilayer membrane and integral channels as supported by both the model and experimental observations. Negative c_0 linearly destabilizes gA channels (Supp Fig. 2B), which agrees with both the SCI (data not shown) and the EB models. Our calculation also shows that $\Delta G_{I,II} \sim (q_L/q_g)^s$, $s = 1, 2$, etc. for 1st, 2nd, etc. order screening, respectively, suggesting that channel formation is harder in charge lipid containing bilayers [30].

In Alm channels the monomers align across the cylindrical surface with many possible conductance states (Supp Fig. 1B) [9,20]. V_{sc} (Eq. (1)) is identical for every Alm monomer accounting for two such screened interactions in both ends. The interactions between Alm monomers follow the Lennard–Jones and Coulomb energy formulas [9,20]. Initiation of observable Alm channel activity requires a certain Alm peptide concentration $[M_A]$ but once channels start showing up, the activity increases rapidly ($\sim[M_A]^{2.6}$ at 25 °C [31]). These data agree with our prediction on channel activity depending mainly on $\Delta G_{I,II}$ in initiation phase, then critically depending on bilayer parameters determining $\Delta G_{I,II}$ (activity sharply increases with $[M_A]$). Similarly to gA, Alm channel activity also shows strong dependence on d_0, c_0 and q_L. $\Delta G_{I,II}$ changes exponentially between different lipid orders [9,20] which can be compared with the compensation of free energy changes [32] due to higher order $[M_A]$ (or $[M_g]$ for gA channels) with increasing d_0 or increasing negative lipid curvature. A brief summary is presented with Supp Fig. 4 and details in [9,20].

Fig. 2 shows the MD results using five AMP–lipid complexes as initial structures as shown in the inset. It plots the separation distance of centers of mass of AMP and lipid molecules, $d_{AMP-lipid}$, against simulation time t (ns). Note that $d_{AMP-lipid}$ was used as the simplest property to quantify the effects of AMP-lipid interactions. $d_{AMP-lipid}$ fluctuates around 10 Å, similarly to the initial setting in two to three simulations in gA-PC, Alm-PC and gA-PS, Alm-PS. AMPs and lipids were observed to be gradually separated.

The solvent accessible (SA) area of the complex was used to investigate whether the hydrophobic effects contribute to AMP–lipid binding. When both AMP and lipid molecules are completely separated we can expect them to be entirely exposed to solvent, i.e., the corresponding SA areas are at a maximum. The Fig. 3 shows that the SA areas in all four cases are unchanged between the start and the investigated 18 Å length. This suggests that within this range the drug lipid complexes stay at an equilibrium solvation condition.

Histograms of $d_{AMP-lipid}$ from all five 10 ns simulations and the corresponding energy contributions from two non-bonded interactions, van der Waals (E_{vdW}) and electrostatic energies (E_{ES}) versus $d_{AMP-lipid}$ are shown in Fig. 4. Both gA and Alm spent more than 2 ns within 6 Å < $d_{AMP-lipid}$ < 12 Å and away from lipids most of the time (see the upper panels in Fig. 4). It suggests the possibility for AMPs to briefly bind with lipids. Fig. 4 (top panel) indicates that gA likely favors the interaction with PC over PS while Alm shows no significant lipid specific preference. Both E_{ES} and E_{vdW} for gA and Alm interacting with PC are roughly inversely proportional to $d_{AMP-lipid}$ while there are weak trends in either gA-PS or Alm-PS cases. E_{ES} and E_{vdW} are strongly effective within 12 Å (E_{vdW} slightly dominant except gA-PS case, see the inset plots of Fig. 4). Both E_{ES} and E_{vdW} are larger for gA than for Alm (see difference in y-axis ranges).

MD simulation detects SCI model predicted ES and vdW energies which have historically been found to originate from the electrical charge properties of the participating agents.

4. Conclusion

The SCI model is found to be an extension of the elastic model that accounts for non-linear effects in the case of large deformations. It has been found to be consistent with the experimental results for two structurally different ion channel functions in varied model membrane systems. Results from our molecular dynamics simulations of both gA (also in [39]) and Alm in lipid membranes confirm that both peptides experience ES and vdW interactions with lipids in membranes. These simulation results importantly suggest that the charge based ES and vdW energies are in fact the primary contributors into the binding energetics. These charge-based energies are found to originate in SCI model based calculations and through numerical computation they have produced necessary binding energetics. Importantly, the much appreciated elastic coupling energy which represents nothing but the mechanical lipid bilayer – channel coupling energy appears naturally in the SCI treatment of the binding energy calculations. We postulate that the SCI plays the most important role in the channel bilayer interactions and the bilayer's inherited elastic properties help the membrane to deform near the channel interface to create physical channel bilayer binding. Charge based interactions are found to be responsible behind creation of driving forces that pull the participating agents to each other's proximity. The energetic picture on the bilayer-channel hydrophobic mismatch regulation of channel function provides new insights into the underlying mechanisms of channel formation by membrane proteins or antimicrobial peptides involved in trans-membrane transport properties. We hope this result will facilitate drug design for various diseases linked to ion channel aberrations.

Acknowledgments

M.A. acknowledges funding (Grant No. 12-MED2670-02) from the National Plan for Science, Technology and Innovation, Saudi Arabian Government. The simulations were conducted using Pharmamatrix high-throughput virtual screening cluster (University of Alberta) and the facilities of the Shared Hierarchical Academic Research Computing Network (SHARCNET: www.sharcnet.ca) and Compute/Calcul Canada.

Appendix A. Supplementary data

Supplementary data associated with this article can be found, in the online version, at http://dx.doi.org/10.1016/j.bbrc.2014.02.012.

References

[1] P.N.T. Unwin, P.D. Ennis, Two configurations of a channel-forming membrane protein, Nature 307 (1984) 609–613.
[2] J.N. Israelachvili, Refinement of the fluid-mosaic model of membrane structure, Biochim. Biophys. Acta 469 (1977) 221–225.

[3] W. Helfrich, Elastic properties of lipid bilayers: theory and possible experiments, Z. Naturforsch. 28C (1973) 693–703.
[4] A.M. O'Connell, R.E. Koeppe II, O.S. Andersen, Kinetics of gramicidin channel formation in lipid bilayers: trans-membrane monomer association, Science 250 (1990) 1256–1259.
[5] G. Boheim, Statistical analysis of alamethicin channels in black lipid membranes, J. Membr. Biol. 19 (1974) 277–303.
[6] K. He, S.J. Ludtke, H.W. Huang, D.L. Worcester, Antimicrobial peptide pores in membranes detected by neutron in-plane scattering, Biochemistry 34 (1995) 15614–15618.
[7] M. Ashrafuzzaman, M.A. Lampson, D.V. Greathouse, R.E. Koeppe II, O.S. Andersen, Manipulating lipid bilayer material properties by biologically active amphipathic molecules, J. Phys. 18 (2006) S1235–S1255.
[8] O.S. Andersen, R.E. Koeppe II, Bilayer thickness and membrane protein function: an energetic perspective, Annu. Rev. Biophys. Biomol. Struct. 36 (2007) 107–130.
[9] M. Ashrafuzzaman, J. Tuszynski, Regulation of channel function due to coupling with a lipid bilayer, J. Comput. Theor. Nanosci. 9 (2012) 564–570.
[10] B.A. Wallace, W.R. Veatch, E.R. Blout, Conformation of gramicidin A in phospholipid vesicles: circular dichroism studies of effects of ion binding, chemical modification, and lipid structure, Biochemistry 20 (1981) 5754–5760.
[11] T.W. Allen, O.S. Andersen, B. Roux, Energetics of ion conduction through the gramicidin channel, Proc. Natl. Acad. Sci. USA 101 (2004) 117–122.
[12] F. de Meyer, B. Smit, Comment on "cluster formation of trans-membrane proteins due to hydrophobic mismatching", Phys. Rev. Lett. 102 (2009) 219801.
[13] H.W. Huang, Deformation free energy of bilayer membrane and its effect on gramicidin channel lifetime, Biophys. J. 50 (1986) 1061–1071.
[14] P. Helfrich, E. Jakobsson, Calculation of deformation energies and conformations in lipid membranes containing gramicidin channels, Biophys. J. 57 (1990) 1075–1084.
[15] J.T. Durkin, L.L. Providence, R.E. Koeppe II, O.S. Andersen, Energetics of heterodimer formation among gramicidin analogues with an NH_2-terminal addition or deletion consequences of missing a residue at the join in the channel, J. Mol. Biol. 231 (1993) 1102–1121.
[16] C. Nielsen, M. Goulian, O.S. Andersen, Energetics of inclusion-induced bilayer deformations, Biophys. J. 74 (1998) 1966–1983.
[17] C. Nielsen, O.S. Andersen, Inclusion-induced bilayer deformations: effects of monolayer equilibrium curvature, Biophys. J. 79 (2000) 2583–2604.
[18] J.A. Lundbæk, P.H.A.J. Birn, R. Søgaard, C. Nielsen, J. Girshman, M.J. Bruno, S.E. Tape, J. Egebjerg, D.V. Greathouse, G.L. Mattice, R.E. Koeppe II, O.S. Andersen, Regulation of sodium channel function by bilayer elasticity. The importance of hydrophobic coupling. Effects of micelle-forming amphiphiles and cholesterol, J. Gen. Physiol. 123 (599–621) (2004) 599–621.
[19] S.M. Gruner, Intrinsic curvature hypothesis for biomembrane lipid composition: a role for nonbilayer lipids, Proc. Natl. Acad. Sci. USA 82 (1985) 3665–3669.
[20] M. Ashrafuzzaman, J. Tuszynski, Membrane Biophysics, Springer, Heidelberg, 2012.
[21] T.C. Hwang, R.E. Koeppe II, O.S. Andersen, Genistein can modulate channel function by a phosphorylation-independent mechanism: importance of hydrophobic mismatch and bilayer mechanics, Biochemistry 42 (2003) 13646–13658.
[22] P.E. Harper, D.A. Mannock, R.N.A.H. Lewis, R.N. McElhaney, S.M. Gruner, X-ray diffraction structures of some phosphatidylethanolamine lamellar and inverted hexagonal phases, Biophys. J. 81 (2001) 2693–2706.
[23] T.K. Rostovtseva, V.M. Aguilella, I. Vodayanoy, S.M. Bezrukov, A. Parsegian, Membrane surface-charge titration probed by gramicidin A channel conductance, Biophys. J. 75 (1998) 1783–1792.
[24] A. Parsegian, Energy of an ion crossing a low dielectric membrane: solutions to four relevant electrostatic problems, Nature 221 (1969) 844–846.
[25] M. Ashrafuzzaman, H. Beck, in: Vortex dynamics in two-dimensional Josephson junction arrays, University of Neuchatel, <http://doc.rero.ch/record/2894?ln=fr>, 2004, p 85 (Chapter 5).
[26] N. Gronbech-Jensen, R.J. Mashl, R.F. Bruinsma, W.M. Gelbart, Counterion-induced attraction between rigid polyelectrolytes, Phys. Rev. Lett. 78 (1997) 2477–2480.
[27] M.T. Lee, W.C. Hung, F.Y. Chen, H.W. Huang, Many-body effect of antimicrobial peptides: on the correlation between lipid's spontaneous curvature and pore formation, Biophys. J. 89 (2005) 4006–4016.
[28] M. Goulian, O.N. Mesquita, D.K. Fygenson, C. Nielsen, O.S. Andersen, Gramicidin channel kinetics under tension, Biophys. J. 74 (1998) 328–337.
[29] J.A. Lundbæk, O.S. Andersen, Spring constants for channel-induced lipid bilayer deformations. Estimates using gramicidin channels, Biophys. J. 76 (1999) 889–895.
[30] S.M. Bezrukov, R.P. Rand, I. Vodyanoy, V.A. Parsegian, Lipid packing stress and polypeptide aggregation: alamethicin channel probed by proton titration of lipid charge, Faraday Discuss. 111 (1998) 173–183.
[31] M. Latorre, O. Alvarez, Voltage-dependent channels in planar lipid bilayer membranes, Physiol. Rev. 61 (1981) 77–150.
[32] Y. Wu, K. He, S.J. Ludtke, H.W. Huang, X-ray diffraction study of lipid bilayer membranes interacting with amphiphilic helical peptides: diphytanoyl phosphatidylcholine with alamethicin at low concentrations, Biophys. J. 68 (1995) 2361–2369.
[33] M. Ashrafuzzaman, C.-Y. Tseng, M. Duszyk, J. Tuszynski, Chemotherapy drugs form ion pores in membranes due to physical interactions with lipids, Chem. Biol. Drug Des. 80 (2012) 992–1002.
[34] D.A. Case, T.A. Darden, T.E. Cheatham III, C.L. Simmerling, J. Wang, et al., AMBER 11, University of California, San Francisco, USA, 2010.
[35] J. Wang, W. Wang, P.A. Kollman, D.A. Case, Automatic atom type and bond type perception in molecular mechanical calculations, J. Mol. Graph. Model. 25 (2006) 247–260.
[36] J. Wang, R.M. Wolf, J.W. Caldwell, P.A. Kollman, D.A. Case, Development and testing of a general AMBER force field, J. Comput. Chem. 25 (2004) 1157–1174.
[37] J.T. Huzil, J. Mane, J.A. Tuszynski, Computer assisted design of second generation colchicine derivatives, Interdiscip. Sci. – Comput. Life Sci. 2 (2010) 169–174.
[38] H. Freedman, J.T. Huzil, T. Luchko, R.F. Luduena, J.A. Tuszynski, Identification and characterization of an intermediate taxol binding site within microtubule nanopores and a mechanism for tubulin isotype binding selectivity, J. Chem. Info. Model. 49 (2009) 424–436.
[39] T.B. Woolf, B. Roux, Molecular dynamics simulation of the gramicidin channel in a phospholipid bilayer, Proc. Natl. Acad. Sci. USA 91 (1994) 11631–11635.